VERTICAL MOMENTUM TRANSFER BY INTERNAL WAVES WITH REGARD FOR THE HORIZONTAL COMPONENT OF ANGULAR VELOCITY OF THE EARTH'S ROTATION

© 2025 A. A. Slepyshev

Marine Hydrophysical Institute of the Russian Academy of Sciences, Sevastopol, Russia

e-mail: slep55@mail.ru

Received September 18, 2024

Revised March 18, 2025

Accepted March 21, 2025

Abstract. Free internal waves in a uniformly stratified fluid are considered in the Boussinesq approximation with regard for the Earth's rotation. It is shown that the dispersion relation, derived with taking into account the horizontal component of the angular velocity of the Earth's rotation at constant wave frequency, is reduced to the canonical equation for second-order curves in the plane of horizontal wave numbers. If the wave frequency is higher than the inertial frequency and less than the Brunt-Väisälä frequency, the frequency isolines are ellipses. If the wave frequency is higher than the buoyancy frequency, then the frequency isolines are hyperbolas; and if the wave frequency is equal to the Brunt-Väisälä frequency, then the isolines are two straight lines parallel the direction to the east. The vertical wave momentum fluxes are obtained as functions of the direction of wave propagation. It is shown that the fluxes are maximum in absolute value when the wave propagates to the north or to the south. A comparison of the vertical momentum fluxes of internal and sub-inertial waves at the same length and the maximum wave amplitude is carried out. It is shown that the vertical momentum flux of sub-inertial waves is higher than that of internal waves and weakens with weakening of stratification.

Keywords: *internal waves, sub-inertial waves, vertical wave momentum flux, Coriolis force*

DOI: 10.31857/S10247084250309e2

INTRODUCTION

The diurnal rotation of the Earth affects ocean dynamics. Currents and internal waves are subject to the Coriolis force. Usually, only the component normal to the Earth's surface of the

angular velocity of its rotation is taken into account in determining the Coriolis force. Such an approximation is called the traditional approximation [1-7]. In the non-traditional approximation, i.e., when the horizontal component of the angular velocity of the Earth's rotation is taken into account, a series of new effects arise, which are noticeably manifested at weak stratification. With respect to the dispersion characteristics of internal waves, this issue is well enough developed [1-7]. At strong stratification, when the buoyancy frequency is much larger than the inertial frequency, the rejection of the traditional approximation practically does not affect the dispersion curves. At weak stratification, when the horizontal component of the Earth's angular velocity is taken into account, the existence of internal waves with a frequency less than the inertial frequency is possibly possible; they are called subinertial internal waves. The frequency range of these waves is wider the smaller the buoyancy frequency. The upper quasi-homogeneous and bottom weakly stratified layers of the sea are the waveguides for these waves. When the frequency of a subinertial wave is reduced to an extremely low frequency, the scale of the wave tends to zero, indicating the possibility of energy dissipation on small scales, for example, during the propagation of subinertial internal waves on horizontally inhomogeneous currents or due to the influence of theβ -effect [1, 6, 8]. In this work, we will consider the effect of the unconventional approximation on vertical momentum transfer by internal waves. Previously, this issue was considered in the traditional approximation in the presence of shear currents [9-11]. It was shown that if the component of the flow velocity normal to the direction of propagation of a normal modes wave depends on the vertical coordinate, the vertical wave momentum fluxes are different from zero when the Earth's rotation is taken into account. Internal waves propagate often in the form of wave packets [12, 13]. Nonlinear effects in the propagation of internal wave packets manifest themselves in the generation of mean currents on the time scale of the wave [14, 15]. The vertical component of the velocity of this induced current at the leading and trailing fronts of the packet has different signs and, as a result, there is no vertical transport [14]. However, there is horizontal transport, which can manifest itself in the transport of suspended sediment and sedimentary material from the shelf to the deep sea.

According to existing concepts, small-scale turbulence is responsible for vertical exchange. Internal waves and shear currents are the source of energy supply for small-scale turbulence in the stratified ocean strata [16-19]. But not only small-scale turbulence is responsible for vertical exchange. When turbulent toughness and diffusion are taken into account, internal waves are damped and the vertical wave fluxes of heat, salt, and momentum are different from zero and contribute to vertical exchange [20, 21]. However, even in the absence of turbulent toughness and diffusion, the vertical wave fluxes of momentum when Earth rotation is taken into account in the traditional approximation are different from zero in the presence of currents with vertical velocity

strike-slip fault [9-11]. It is of interest to study the effect of rejection of the traditional approximation on vertical momentum transport by internal waves for strong and weak stratification, when subinertial internal waves play a significant role.

1. PROBLEM STATEMENT

Free internal waves in a boundless vertically stratified basin of constant depth are considered, taking into account the contribution of the horizontal component of the Earth's angular velocity to the Coriolis force. The dispersion relation is found in the linear approximation and the boundary value problem for the amplitude of the vertical velocity of internal shafts at constant buoyancy frequency is solved. Secondly, the vertical wave momentum fluxes are found in the second order by the wave amplitude.

The system of equations of hydrodynamics in the Boussinesq approximation [4, 22] for wave perturbations has the form:

$$\frac{Du}{Dt} + f_c w - fv = -\frac{1}{\bar{\rho}_0}\frac{\partial P}{\partial x} \tag{1.1}$$

$$\frac{Dv}{Dt} + fu = -\frac{1}{\bar{\rho}_0}\frac{\partial P}{\partial y} \tag{1.2}$$

$$\frac{Dw}{Dt} - f_c u = -\frac{1}{\bar{\rho}_0}\frac{\partial P}{\partial z} - \frac{g\rho}{\bar{\rho}_0} \tag{1.3}$$

$$\frac{\partial u}{\partial x} + \frac{\partial v}{\partial y} + \frac{\partial w}{\partial z} = 0 \tag{1.4}$$

$$\frac{D\rho}{Dt} + w\frac{\partial \rho_0}{\partial z} = 0 \tag{1.5}$$

$$f = 2\Omega \sin\varphi, \quad f_c = 2\Omega\cos\varphi$$

where Ω - angular velocity of Earth rotation, φ - latitude, f - Coriolis parameter - inertial frequency; axis x is directed eastward, axis y northward, axis z is directed vertically upward; u, v, w - respectively two horizontal and vertical components of wave perturbations of flow velocity along these axes, P and ρ - wave perturbations of pressure and density, $\rho_0(z)$ - unperturbed mean density, $\bar{\rho}_0$ - its depth-averaged value, constant value in the Boussinesq approximation; the action of operator D/Dt is revealed by formula $\frac{D}{Dt} = \frac{\partial}{\partial t} + u\frac{\partial}{\partial x} + v\frac{\partial}{\partial y} + w\frac{\partial}{\partial z}$.

Boundary conditions at the sea surface ($z = 0$) are the "hard cap" condition that filters out internal waves from surface waves [4, 22]: $w(0) = 0$. Boundary conditions at the bottom are the "no-flow" condition: $w(-H) = 0$, H - Sea depth.

2. LINEAR APPROXIMATION

Solutions of the system (1.1)-(1.5) in the linear approximation are sought in the form:

$$u = u_{10}(z)Ae^{j\theta} + \text{c.c.}, \quad v = v_{10}(z)Ae^{j\theta} + \text{c.c.}, \quad w = w_{10}(z)Ae^{j\theta} + \text{c.c.}$$

$$P = P_{10}(z)Ae^{j\theta} + \text{c.c.}, \quad \rho = \rho_{10}(z)Ae^{j\theta} + \text{c.c.}, \tag{2.1}$$

where c.c. - complex-conjugate summands, A - amplitude multiplier; θ - wave phase, $\theta = kx + ly - \omega t$; k, l - horizontal wave numbers, projections of the wave vector $\vec{k}_h$ on the x, y axes, respectively; ω - wave frequency.

Substituting (2.1) into the system (1.1)-(1.5) we find the relationship of amplitude functions u_{10}, v_{10}, ρ_{10}, P_{10} with w_{10} and the equation for the w_{10}

$$u_{10} = \frac{\frac{dw_{10}}{dz}(ik\omega - fl) - if_c l^2 w_{10}}{\omega\left(k^2 + l^2\right)} \tag{2.2}$$

$$v_{10} = \frac{\frac{dw_{10}}{dz}(fk + il\omega l) + if_c l k w_{10}}{\omega\left(k^2 + l^2\right)} \tag{2.3}$$

$$\frac{P_{10}}{\bar{\rho}_0} = \frac{i\frac{dw_{10}}{dz}\left(\omega^2 - f^2\right) + f_c(ik\omega + fl)w_{10}}{\omega\left(k^2 + l^2\right)}$$

$$\rho_{10} = -\frac{i}{\omega} w_{10} \frac{d\rho_0}{dz}$$

The function w_{10} satisfies the equation [3, 4, 6]

$$\frac{d^2 w_{10}}{dz^2} + a(z)\frac{dw_{10}}{dz} + b(z)w_{10} = 0 \tag{2.4}$$

where $a(z) = -\frac{2ilff_c}{\omega^2 - f^2}$, $b(z) = \frac{\left(N^2 - \omega^2\right)\left(k^2 + l^2\right) + f_c^2 l^2}{\omega^2 - f^2}$,

$N^2 = -\frac{g}{\bar{\rho}_0}\frac{d\rho_0}{dz}$ - the square of the Brent-Wäisälä frequency.

Boundary conditions for w_{10}

$$w_{10}(0) = w_{10}(-H) = 0. \tag{2.5}$$

3. MOMENTUM WAVE STREAMS

It is of interest to find the projections of wave perturbations of the flow velocity to the directions along and across the horizontal wave vector $\mathbf{k}_h$. Obviously $k_h^2 = \left(k^2 + l^2\right)$. Let α be the angle of the wave vector $\mathbf{k}_h$ with the axis x. A positive value of the angle α corresponds to a counterclockwise rotation of the axis x to the vector $\mathbf{k}_h$. Let us introduce a coordinate system rotated in the horizontal plane by this angle α x', y'. The axis x' is directed along the vector $\mathbf{k}_h$, the axis y' is perpendicular to it. Then the projections of wave perturbations of the flow velocity on the x', y' axes are as follows:

$$u' = u\cos\alpha + v\sin\alpha, \qquad v' = v\cos\alpha - u\sin\alpha$$

From the representation of solutions for u, v as (2.1), it follows that u', v' can be represented as

$$u' = u'_1(z)Ae^{i\theta} + \text{c.c.}, \quad v' = v'_1(z)Ae^{i\theta} + \text{c.c.} \tag{3.1}$$

where u'_1, v'_1 are determined by formulas:

$$u'_1 = u_{10}\cos\alpha + v_{10}\sin\alpha, \qquad v'_1 = v_{10}\cos\alpha - u_{10}\sin\alpha \tag{3.2}$$

From relations (3.1), (3.2) and (2.2). (2.3) we find the vertical wave fluxes of momentum

$$\overline{u'w} = \frac{i}{k_h}\left|A^2\right|\left(w_{10}^{*}\frac{dw_{10}}{dz} - w_{10}\frac{dw_{10}^{*}}{dz}\right) \tag{3.3}$$

$$\overline{v'w} = \frac{f}{\omega k_h}\left|A^2\right|\frac{d\left(w_{10}w_{10}^{*}\right)}{dz} \tag{3.4}$$

Here the line at the top means averaging over the period of the wave. The vertical wave flux of momentum $\overline{v'w}$ is different from zero when the Earth's rotation is taken into account. The boundary value problem (2.4), (2.5) has complex coefficients at $l \neq 0$ and complex solutions. Therefore, the flux $\overline{u'w}$ (3.3) is not zero when the horizontal component of the Earth's angular velocity is taken into account. In the traditional approximation, this flux shaft is zero because equation (2.4) at $f_c = 0$ has real coefficients and the solution of the boundary value problem (2.4), (2.5) is a real function. At $\alpha = 0; \pi$ the wave number$l = 0$ and vertical wave momentum flux $\overline{u'w}$ is zero in the non-traditional approximation, since equation (2.4) has valid coefficients and valid solutions and coincides with the equation of the traditional approximation.

The normalizing multiplier$A$ is found from the known value of the maximum amplitude of vertical displacements ζ_{max}. For this purpose, we express the vertical displacement ζ, using the relation: $d\zeta/dt = w$

$$\zeta = \frac{iw_{10}}{\omega}A\exp(ily - i\omega t) + \text{c.c.}$$

Hence

$$A = \frac{\zeta_{max}}{2\max\left|w_{10}/\omega\right|}. \tag{3.5}$$

4. CALCULATION RESULTS

Equation (2.4) admits an exact analytical solution at constant Brent-Väisälä frequency. Then equation (2.4) is simplified to the form:

$$\frac{d^2 w_{10}}{dz^2} + 2ia_0 \frac{dw_{10}}{dz} + b_0 w_{10} = 0 \tag{4.1}$$

$$\text{where } a_0 = -\frac{lff_c}{\omega^2 - f^2},\ b_0 = \frac{k_h^2}{\omega^2 - f^2}\left(N^2 - \omega^2 + f_c^2 \sin^2\alpha\right) \tag{4.2}$$

The solution of the boundary value problem (4.1), (2.5) has the form:

$$w_{10}(z) = e^{-ia_0 \cdot z} \cdot \sin\left(z\sqrt{a_0^2 + b_0}\right) \tag{4.3}$$

The dispersion equation resulting from the boundary conditions (2.5) is valid at: $z = -H$

$$H\sqrt{a_0^2 + b_0} = \pi n$$

where n is a positive integer.

Hence.

$$a_0^2 + b_0 = \left(\frac{\pi n}{H}\right)^2 \tag{4.4}$$

After substituting expressions (4.2) for a_0, b_0 into (4.4) we obtain

$$\frac{f^2 f_c^2 k_h^2 \sin^2\alpha}{\left(\omega^2 - f^2\right)^2} + \frac{k_h^2}{\omega^2 - f^2}\left[N^2 - \omega^2 + f_c^2 \sin^2\alpha\right] = \left(\frac{\pi n}{H}\right)^2 \tag{4.5}$$

Hence the dispersion relation [3, 4, 6]:

$$k_h^2 = \frac{\left(\frac{\pi n}{H}\right)^2 \left(\omega^2 - f^2\right)^2}{\left(N^2 - \omega^2\right)\left(\omega^2 - f^2\right) + \omega^2 f_c^2 \sin^2\alpha} \tag{4.6}$$

Here n is the mode number. It is easy to see that in the traditional approximation at $f_c = 0$ the dispersion relation (4.6) transforms into the known relation at a constant Brent-Väisälä frequency [4, 5, 22]:

$$\omega^2 = \frac{N^2 k_h^2 + f^2\left(\frac{\pi n}{H}\right)^2}{k_h^2 + \left(\frac{\pi n}{H}\right)^2},\ k_h^2 = \frac{\left(\frac{\pi n}{H}\right)^2 \left(\omega^2 - f^2\right)}{\left(N^2 - \omega^2\right)} \tag{4.7}$$

From the positivity condition k_h^2 (4.7) follows the inequality $f^2 < \omega^2 < N^2$ at $N > f$, i.e., for internal shafts in the traditional approximation, the wave frequency satisfies the inequality $f < \omega < N$.

When the horizontal component of the Earth's angular velocity is taken into account, the condition of positivity k_h^2 (4.6) leads to the inequality for the frequency ω [3, 4, 6]:

$$\omega_2^2 < \omega^2 < \omega_1^2 \tag{4.8}$$

where ω_1, ω_2 are determined by formulas [3, 4, 6]:

$$\omega_{1,2}^2 = \frac{1}{2}\left[N^2 + f^2 + f_c^2 \sin^2\alpha \pm \sqrt{\left(N^2 - f^2\right)^2 + f_c^4 \sin^4\alpha + 2 f_c^2 \sin^2\alpha \left(N^2 + f^2\right)} \right] \tag{4.9}$$

It should be noted the validity of the following inequalities [3]:

$$\omega_1^2 > \max\left(N^2, f^2\right); \qquad \omega_2^2 < \min\left(N^2, f^2\right) \tag{4.10}$$

It is not difficult to see that the dispersion equation (4.6) at a fixed wave frequencyω is equivalent to the canonical equation (4.11) for second-order curves in the plane of horizontal wave numbers k, l (the corresponding proof is given in the Appendix):

$$\frac{k^2}{a^2} + \frac{l^2}{b^2} = 1 \tag{4.11}$$

where

$$a^2 = \frac{\left(\frac{\pi n}{H}\right)^2 \left(\omega^2 - f^2\right)}{\left(N^2 - \omega^2\right)}; \qquad b^2 = \frac{\left(\frac{\pi n}{H}\right)^2 \left(\omega^2 - f^2\right)^2}{\left(N^2 - \omega^2\right)\left(\omega^2 - f^2\right) + \omega^2 f_c^2} \tag{4.12}$$

Equation (4.11) at $a^2 > 0$ is the equation of an ellipse, since at this and $b^2 > 0$, a is the major semi-axis of the ellipse, b is the minor semi-axis. When $a^2 < 0$ and $b^2 > 0$, equation (4.11) is the equation of a hyperbola. If $1/a^2 = 0$ (at $\omega = N$), equation (4.11) becomes the equation of two lines parallel to the axis k:

$$l = \pm \frac{\pi n \left(N^2 - f^2\right)}{HNf_c} \tag{4.13}$$

Consider the case $N > f$, $\omega > f$, corresponding to internal waves. At $f < \omega < N$ equation (4.11) is the equation of an ellipse, at $\omega > N$ and $b^2 > 0$ equation (4.11) is the equation of a hyperbola. The solution of the inequality $b^2 > 0$ has the form:

$$\omega_{2*}^2 < \omega^2 < \omega_{1*}^2 \tag{4.14}$$

where ω_{2*}^2, ω_{1*}^2 are determined by formulas:

$$\omega_{1,2*}^2 = \frac{1}{2}\left[N^2 + f^2 + f_c^2 \pm \sqrt{\left(N^2 - f^2\right)^2 + f_c^4 + 2f_c^2\left(N^2 + f^2\right)} \right] \tag{4.15}$$

It is not difficult to see that inequality (4.14) coincides with inequality (4.8) at $\sin^2\alpha = 1$, with ω_{2*}^2, ω_{1*}^2 satisfying conditions (4.10), i.e., the conditions are satisfied:

$$\omega_{1*}^2 > N^2 \qquad \omega_{2*}^2 < f^2 \tag{4.16}$$

Hence the inequality $b^2 > 0$ is satisfied at

$$N^2 < \omega^2 < \omega_{1*}^2 \tag{4.17}$$

Thus, when inequality (4.17) is satisfied, the frequency isolines in the plane of horizontal wave numbers are hyperbolas.

Further analysis of wave frequency isolines in the plane of horizontal wave numbers will be carried out for internal waves of the firstly mode ($n = 1$) with frequency ω, satisfying the condition $f < \omega < \omega_{1*}$ for three types of stratification: $N_1 = 3$ cycle/h - strong stratification; $N_2 = 2.5f$ - weak stratification; $N_3 = 1.5f$ - very weak stratification. Sea depth $H = 200$ m, latitude $\varphi = 44.8°$ north latitude. In the traditional approximation, the wave frequency isolines in the plane of horizontal wave numbers are circles, the square of the radius of which is determined by formula (4.7). Figure 1 shows the wave frequency isolines in the plane of horizontal wave numbers at strong stratification when the horizontal component of the Earth's angular velocity of rotation is taken into account. In the case of strong stratification at $f < \omega < 0.98N_1$ in Fig. 1, the ellipses turn into circles, almost coinciding with circles in the traditional approximation. The frequency $\omega = 0.98N_1$ corresponds to a wavelength of 57.6 m, for longer wavelengths the frequency isolines are circles. In the frequency interval $0.98N_1 \le \omega < N_1$ frequency isolines are ellipses.

At $\omega = N_1$ the isolines in Figure 1 are straight lines $l = \pm\frac{\pi\left(N_1^2 - f^2\right)}{HN_1 f_c}$, at $N_1 < \omega < \omega_{1^*}$ the isolines are hyperbolas.

Figure 2 shows the wave frequency isolines in the plane of horizontal wave numbers at weak stratification when . $N_2 = 2.5f$

The closed lines in Fig. 2 are ellipses. At these frequencies at strong stratification the frequency isolines are circles. At$\omega = N_2$ the isolines in Fig. 2 are straight lines (4.13), at$N_2 < \omega < \omega_{1^*}$ the isolines are hyperbolas.

Fig. 3 shows the wave frequency isolines in the plane of horizontal wave numbers at very weak stratification when $N_2 = 2.5f$.

In general, the picture of frequency isolines at very weak stratification is similar to the same picture for weak stratification, but in the vicinity of the origin, the ellipses at very weak stratification are more flattened to the abscissa axis than at weak stratification, i.e., the anisotropy of closed frequency isolines increases with weakening of stratification. Note that at $\sin\alpha = 0$ the dispersion relation (4.6) transforms into the relation (4.7) in the traditional approximation, and the major semi-axis of the ellipse a in (4.12) is equal to the radius k_h of the circle of the frequency isoline in the traditional approximation, i.e. waves running to the east or to the west do not experience any influence on the variance from taking into account the horizontal component of the Earth's angular velocity. But the influence is maximized for waves running north or south.

It should be noted that the solution (4.3) of the boundary value problem (4.1), (2.5) using (4.4) can be represented in the form:

$$w_{10}(z) = e^{-ia_0 \cdot z} \cdot \sin\left(\frac{\pi n z}{H}\right) \tag{4.18}$$

(Hence the vertical wave momentum fluxes) ((3.3), (3.4) () are of the form:)

$$\overline{u'w} = -2\left|A^2\right|\frac{f \cdot f_c}{\omega^2 - f^2} \cdot \sin\alpha \cdot \sin^2\left(\frac{\pi n z}{H}\right), \tag{4.19}$$

$$\overline{v'w} = \frac{\left|A^2\right| f}{\omega k_h}\frac{\pi n}{H}\sin\left(\frac{2\pi n z}{H}\right). \tag{4.20}$$

Calculations of the vertical wave fluxes of momentum (4.19) and (4.20) at internal waves of the first mode with the maximum amplitude $\zeta_{max} = 2$ m are performed for the three considered types of stratification. In Fig. 4 *a* presents the profiles of the vertical pulse flux $\overline{u'w}$ (4.19) at strong stratification for first mode internal waves with frequency $0.8 \cdot N_1$ for four values of angle α: $\alpha_1 = 0; \alpha_2 = \pi/6; \alpha_3 = \pi/3; \alpha_4 = \pi/2$. With increasing angleα the pulse flux increases in modulus

and reaches its maximum value at $\alpha_4 = \pi/2$. The pulse flux at $\alpha = \pi - \alpha_i$ ($i = 1, 2, 3, 4$) coincide with the pulse fluxes at $\alpha = \alpha_i$. At negative angles $\alpha = -\alpha_i$ the sign of the pulse flux $\overline{u'w}$ is reversed.

In the traditional approximation, the momentum flux $\overline{u'w}$ (4.19) is zero, since $f_c = 0$.

The vertical wave flux of the pulse $\overline{v'w}$ (4.20) in Fig. 4 b for the wave frequency $0.8 \cdot N_1$ at strong stratification does not depend practically on the angleα and coincides with the flux of the traditional approximation.

Fig. 5 shows the vertical wave flux profiles of the pulse at weak stratification ($N_2 = 2.5f$) for the first mode wave with frequency $\omega = 1.4f$ with maximum amplitude $\zeta_{max} = 2$ m.

The dependence of the vertical pulse wave fluxes on the angleα in Fig. 5a essentially repeats the same dependence as in Fig. 4a, only the magnitudes of the fluxes are modulo higher at the same wave amplitude. The vertical wave flux of the pulse $\overline{v'w}$ in Fig. 5b at weak stratification already depends on the angle, reaches its maximum modulo value at $\alpha_4 = \pm\pi/2$ and coincides with the flux of the conventional approximation at $\alpha = 0, \pi$. The momentum flux at $\alpha = \pi - \alpha_i$ ($i = 1, 2, 3, 4$) coincide with the momentum flux at $\alpha = \alpha_i$. When the sign of the angle α changes, the momentum flux $\overline{v'w}$ does not change. The momentum flux $\overline{v'w}$ at weak stratification is weaker than the flux at strong stratification.

Fig. 6 shows the vertical wave flux profiles of the pulse at very weak stratification ($N_3 = 1.5f$) for the first mode wave with frequency $\omega = 1.4f$ with maximum amplitude $\zeta_{max} = 2$ m.

The momentum flows in Fig. 6 qualitatively repeat the flows in Fig. 5, only the angle dependence is stronger. The momentum fluxes of $\overline{v'w}$ in Fig. 6b is smaller modulo the fluxes in Fig. 5b, while the $\overline{u'w}$ momentum fluxes in Fig. 5a are identical to the fluxes in Fig. 6a. This is explained by the fact that the expression (4.19) for the $\overline{u'w}$ momentum flux does not include the horizontal wave number k_h, only the frequency, and it is the same for weak and very weak stratification, $\omega = 1.4f$, the normalizing multiplier (3.5) is also the same. It should be noted that the maximum modulo value of the vertical wave momentum fluxes on the closed frequency isoline is reached at $\alpha = \pm\pi/2$, i.e., when the wave propagates north or south. In the traditional approximation, the momentum fluxes do not depend on the direction of wave propagation.

To solve the dispersion equation (4.6) with respect to the frequency of the wave we use equation (4.5):

$$\frac{f^2 f_c^2 k_h^2 \sin^2\alpha}{\left(\omega^2 - f^2\right)^2} + \frac{k_h^2}{\omega^2 - f^2}\left[N^2 - f^2 - \omega^2 + f^2 + f_c^2 \sin^2\alpha\right] = \left(\frac{\pi n}{H}\right)^2$$

Hence.

$$\frac{f^2 f_c^2 k_h^2 \sin^2\alpha}{\left(\omega^2 - f^2\right)^2} - k_h^2 + \frac{k_h^2}{\omega^2 - f^2}\left[N^2 - f^2 + f_c^2 \sin^2\alpha\right] = \left(\frac{\pi n}{H}\right)^2 \qquad (4.21)$$

In equation (4.21) it is convenient to make a substitution:

$$R = \frac{1}{\omega^2 - f^2}$$

From equation (4.21) follows the quadratic equation for R:

$$f^2 f_c^2 \sin^2\alpha \cdot R^2 + R\left(N^2 - f^2 + f_c^2 \sin^2\alpha\right) - 1 - \left(\frac{\pi n}{k_h H}\right)^2 = 0 \qquad (4.22)$$

After the solution of the quadratic equation (4.22) is found ω^2:

$$\omega^2 = f^2 + \frac{2 f^2 f_c^2 \sin^2\alpha}{-\left(N^2 - f^2 + f_c^2 \sin^2\alpha\right) \pm \sqrt{\left(N^2 - f^2 + f_c^2 \sin^2\alpha\right)^2 + 4 f^2 f_c^2 \sin^2\alpha \left(1 + \left(\frac{\pi n}{k_h H}\right)^2\right)}} \qquad (4.23)$$

The positive sign before the square root in (4.23) corresponds to internal waves, which have $f < \omega < \omega_1$, the negative sign corresponds to subinertial waves, which have $\omega_2 < \omega < f$ [1, 3, 4, 6].

Fig. 7 shows the dispersion curves of the first two modes of internal waves and subinertial waves propagating northward for the three stratification types considered. In Fig. 7a at strong stratification, the dispersion curves of the subinertial waves degenerate into a straight line corresponding to a frequency lower than the inertial frequency by the value $2 \cdot 10^{-8}$ rad/s. The detailed behavior of the dispersion curves of subinertial waves in this case in the vicinity of the inertial frequency at small wave numbers is revealed by Fig. 7b, which shows the dependence of the difference $\omega - f$ on the wave number. At $l \to 0$ the difference $\omega - f \to 0$, remains negative. At weak stratification in Fig. 7c the degeneracy is removed and the dispersion curves of the first and second modes of the subinertial waves are already distinguishable. They are even better distinguishable at very weak stratification in Fig. 7г.

It is of interest to compare the vertical wave momentum fluxes of internal and subinertial waves of the first mode propagating northward with the same length $\lambda = 200$ m and maximum amplitude $\zeta_{max} = 2$ m for the three types of stratification considered. Fig. 8 shows the vertical momentum flux profiles $\overline{u'w}$ for internal (1) and subinertial (2) waves for strong (a), weak (b), and very weak stratification (c).

Note the very high vertical momentum flux of the subinertial wave at strong stratification in Fig. 8a, which is on the order of magnitude comparable or higher than the typical turbulent vertical momentum flux. In contrast, the internal wave in Fig. 8a has a weak flux. At the weak

stratification in Fig. 8b, the vertical momentum flux of the subinertial wave is significantly weaker, and in contrast, the internal wave has stronger flux. Nevertheless, the flux of the subinertial wave is modulo higher than that of the internal wave. The same trend holds for the very weak stratification in Fig. 8c. There is a further weakening of the momentum flux at the subinertial wave, while the flux at the internal wave is enhanced (Fig. 8d). Lines *1*, *2*, and *3* in Fig. 8d correspond to strong, weak, and very weak stratification.

A comparison of the vertical wave pulse $\overline{v'w}$ of the internal and subinertial waves of the first mode with wavelength $\lambda = 200$ m and maximum amplitude $\zeta_{max} = 2$ m for strong (a), weak (b), and very weak (c) stratification is shown in Fig. 9. Everywhere, the vertical flux of the $\overline{v'w}$ impulse of the internal wave exceeds in modulus the corresponding flux of the subinertial wave, with the strong stratification in Fig. 9a showing the strongest difference. A general trend of decreasing $\overline{v'w}$ momentum flux with weakening stratification is present. Fig. 9d. shows the vertical wave flux profiles of momentum flux $\overline{v'w}$ at the subinertial wave for the three stratification types considered. Lines *1*, *2*, and *3* in Fig. 9g correspond to strong, weak, and very weak stratification. Stratification affects this momentum flux at the subinertial wave more weakly than the same flux at the internal wave.

CONCLUSION

The equation for the amplitude of the vertical velocity of internal waves when the horizontal component of the Earth's angular velocity is taken into account has a complex coefficient at the first derivative; in the traditional approximation, it is zero. The eigenfunction of internal waves in the non-traditional approximation is complex, although the wave frequency is real. It is shown that the dispersion relation at constant wave frequency reduces to the canonical equation for secondly order curves in the plane of horizontal wave numbers. If the internal wave frequency is greater than the inertial wave frequency but less than the buoyancy frequency, the frequency isolines are ellipses; if the frequency is greater than the buoyancy frequency but less than the maximum possibly frequency, the frequency isolines are hyperbolas. If the frequency of the wave is equal to the buoyancy frequency, the frequency isolines are straight lines parallel to the eastward direction. In the traditional approximation, ellipses become circles with radius equal to the major semi-axis of the ellipse, and there are no straight lines or hyperbolas. The influence of the unconventional approximation on the dispersion curves is the stronger the weaker the stratification.

The vertical wave impulse flux in absolute value in the traditional approximation does not depend on the direction of wave propagation. It is obtained that in the non-traditional approximation it depends on the direction of wave propagation, and the effect is maximum when the wave propagates northward or southward. Then there is a vertical momentum transfer for the

two components of the wave perturbations of the flow velocity along and across the wave propagation direction. Whereas in the traditional approximation, vertical momentum transfer is present only for the velocity component transverse to the direction of wave propagation. It is shown for weak and very weak stratification that in the non-traditional approximation this momentum flux increases in modulus with increasing angle of the wave vector with the eastward direction and reaches its maximum value when the wave propagates northward (or southward). When propagating westward or eastward, it is equal to the flux of the conventional approximation. The effect increases with weakening of stratification, but for strong stratification it is absent and this momentum flux is equal to the flux of the traditional approximation.

ACKNOWLEDGEMENT

The author is grateful to G. S. Kondrashin for help in numerical calculations.

FUNDING

The work was carried out within the framework of the state assignment on the theme FNNN-2021-0004 "Fundamental research of processes determining the flow of matter and energy in the marine environment and at its boundaries, the state and evolution of the physical and biogeochemical structure of marine systems in modern conditions" **(**cipher "Oceanological processes"**).**

The dispersion relation (4.6) has the form

$$k_h^2 = \frac{\left(\frac{\pi n}{H}\right)^2 \left(\omega^2 - f^2\right)^2}{\left(N^2 - \omega^2\right)\left(\omega^2 - f^2\right) + \omega^2 f_c^2 \sin^2\alpha} \tag{P1}$$

It is not difficult to show that equation (P1) at constant wave frequency is equivalent to the canonical equation for second order curves in the plane of horizontal wave k, l numbers of the form

$$\frac{k^2}{a^2} + \frac{l^2}{b^2} = 1 \tag{P2}$$

where

$$a^2 = \frac{\left(\frac{\pi n}{H}\right)^2 \left(\omega^2 - f^2\right)}{\left(N^2 - \omega^2\right)}; b^2 = \frac{\left(\frac{\pi n}{H}\right)^2 \left(\omega^2 - f^2\right)^2}{\left(N^2 - \omega^2\right)\left(\omega^2 - f^2\right) + \omega^2 f_c^2} \tag{P3}$$

Indeed, after substituting a^2 and b^2 (P3) into (P2), we shaft

$$\frac{k^2\left(N^2 - \omega^2\right)}{\left(\frac{\pi n}{H}\right)^2 \left(\omega^2 - f^2\right)} + \frac{l^2\left[\left(N^2 - \omega^2\right)\left(\omega^2 - f^2\right) + \omega^2 f_c^2\right]}{\left(\frac{\pi n}{H}\right)^2 \left(\omega^2 - f^2\right)^2} = 1 \tag{P4}$$

Multiply both parts of (P4) by the denominator of the secondly summand in the left-hand side of the equation

$$k^2\left(N^2 - \omega^2\right)\left(\omega^2 - f^2\right) + l^2\left[\left(N^2 - \omega^2\right)\left(\omega^2 - f^2\right) + \omega^2 f_c^2\right] = \left(\frac{\pi n}{H}\right)^2 \left(\omega^2 - f^2\right)^2$$

Hence.

$$\left(k^2 + l^2\right)\left(N^2 - \omega^2\right)\left(\omega^2 - f^2\right) + l^2\omega^2 f_c^2 = \left(\frac{\pi n}{H}\right)^2 \left(\omega^2 - f^2\right)^2 \tag{P5}$$

Given that $k_h^2 = \left(k^2 + l^2\right), l^2 = k_h^2 \sin^2\alpha$, equation (P5) is transformed to the form

$$k_h^2\left[\left(N^2 - \omega^2\right)\left(\omega^2 - f^2\right) + \omega^2 f_c^2 \sin^2\alpha\right] = \left(\frac{\pi n}{H}\right)^2 \left(\omega^2 - f^2\right)^2$$

Hence.

$$k_h^2 = \frac{\left(\frac{\pi n}{H}\right)^2 \left(\omega^2 - f^2\right)^2}{\left(N^2 - \omega^2\right)\left(\omega^2 - f^2\right) + \omega^2 f_c^2 \sin^2\alpha} \qquad \text{(P6)}$$

Equation (P6) coincides with equation (P1). Thus, equation (P2) is equivalent to the dispersion equation (P1), (4.6).

REFERENCES

1. *Badulin S.I., Vasilenko V.M., Yaremchuk M.I.* On the peculiarities of interpretation of quasi-inertial motions on the example of the data of the Megapolygon experiment // Izv. of the USSR Academy of Sciences. FAO. 1991. V. 27. № 6. P. 638-647.
2. *Saint-Guily B.* On internal waves: Effects of the horizontal component of the Earth's rotation and of a uniform current // Dtsch. Hydrogr. Z. 1970. V. 23. P. 16-23.
3. *Kamenkovich V.M., Kulakov A.V.* To the question about the influence of rotation on waves in the stratified ocean // Oceanology. 1977. № 3. P. 400-410.
4. *Brekhovskikh L.M., Goncharov V.V.* Introduction to mechanics of continuous media. Moscow: Nauka, 1982. 337 p.
5. *Le Blon P., Majsek L.* Waves in the Ocean. M.: Mir, 1981. P. 1. 480 p. P. 2. 363 p.
6. *Gerkema T., Shrira V.I.* Near-inertial waves in the ocean: beyond the traditional approximation // J. Fluid. Fluid. Mech. 2005. V. 52. P. 195-219.
7. *Reznik G.M.* Shaft motions in the stable-neutrally stratified ocean // Oceanology. 2015. V. 55. № 6. P. 875-882.
8. *Gerkema T., Shrira V. I.* Near-inertial waves on the "nontraditional" b-plane // J. Geophys. Geophys. Res. 2005. V.110. C01003. Doi:10.1029/2004JC002519
9. *Slepyshev A.A., Laktionova N.V.* Vertical momentum transfer by internal waves in a shear flow (in Russian) // Izv. RAS. FAO. 2019. V. 55. № 6. P. 194-200.
10. *Vorotnikov D.I., Slepyshev A.A.* Vertical momentum flows caused by weakly nonlinear internal waves on the shelf (in Russian) // Izv. RAS. MZHG. 2018. № 1. P. 23-35.
11. *Ankudinov N.O., Slepyshev A.A.* Vertical momentum transfer by internal waves in a two-dimensional flow (in Russian) // Izv. RAS. MZHG. 2021. № 3. P 39-47.
12. *Bulatov V.V., Vladimirov Y.V.* Waves in stratified media. Moscow: Nauka, 2015. 735 p.
13. *Ivanov V.A., Shulga T.Ya., Bagaev A.V., Medvedeva A.V., Plastun T.V., Vrzhevskaya L.V., Svishcheva I.A.* Internal waves in the area of the Herakleysky Peninsula: modeling and observation// Izv. RAS. IYZH. 2019. V. 35, № 4. P. 322-340. https://doi.org/10.22449/0233-7584-2019-4-322-340

14. *Borisenko Yu.D., Voronovich A.G., Leonov A.I., Miropolsky Yu.Z.* To the theory of unsteady weakly nonlinear internal shafts in a stratified liquid // Izv. of the USSR Academy of Sciences. FAO. I976. V.12. № 3. P. 293-301.
15. *Grimshaw R.* The modulation of an internal gravity wave packet and the resonance with the mean motion // Stud. In Appl. Math. 1977. V. 56. P. 241-266. doi.org/10.1002/sapm1977563241
16. *Samodurov A.S., Lyubitskiy A.A., Panteleev N.A.* Contribution of overturning internal shafts to structure formation, energy dissipation and vertical diffusion in the ocean // Izv. RAS. IYZH. 1994. № 3. P. 14-27.
17. *Podymov O.I., Zatsepin A.G., Ostrovsky A.G.* Vertical turbulent exchange in the Black Sea pycnocline and its relation to the shaft dynamics // Oceanology. 2017. V. 57. № 4. P. 546–559. https://doi.org/10.7868/S0030157417040049
18. *Ivanov A.V., Ostrovsky L.A.,Soustova I.A.,Thimring L.Sh.* Interaction of internal waves and turbulence in the upper layer of the ocean // Dyn. Atm. and Ocean. 1984. V. 3. N. 7. P. 221-232.
19. *Soustova I.A., Troitskaya Y.I.* et al. Simple description of turbulent transport in stratified shear flow applied to the description of thermohydrodynamics of inland reservoirs // Izv. RAS. FAO. 2020. V. 56. № 6. P. 689-699.
20. *Nosova A.V., Slepyshev A.A.* Vertical fluxes induced by weakly nonlinear internal waves on a shelf // Fluid. Dyn. 2015. V. 50. № 1. P. 12-21. DOI: 10.1134/S0015462815010020
21. *Slepyshev, A.A.* Vertical momentum transfer by internal waves under consideration of turbulent toughness and diffusion (in Russian) // Izv. RAS. FAO. 2016. V. 52. № 3. P. 342-349.
22. *Miropol'skiy Yu.Z.* Dynamics of internal gravity waves in the ocean. L.: Gidrometeoizdat, 1981. 302 p.

FIGURE CAPTIONS

Fig. 1. Frequency isolines at strong stratification: *1′–8′* : $\omega = 0.9995N_1$, $0.9999N_1$, $0.99999N_1$, $1.000001943N_1$, $1.000007721N_1$, $1.00001166N_1$, $1.0001846N_1$, $\omega = N_1$.

Fig. 2. Frequency isolines at weak stratification: *1′–8′*: $\omega = 2.4f$, $2.46f$, $0.999N_2$, $1.001N_2$, $1.036N_2$, $1.054N_2$, $1.085N_2$, N_2.

Fig. 3. Frequency isolines at very weak stratification: *1′–8′*: $\omega = 1.34f$, $1.44f$, $0.994N_3$, $1.003N_3$, $1.109N_3$, $1.116N_3$, $1.126N_3$, N_3.

Fig. 4. Vertical pulse wave flux profiles of $\overline{u'w}$ (a) and $\overline{v'w}$ (b) at different values ofα angle for strong stratification: $\alpha_1 = 0$ (*1′*); $\alpha_2 = \pi/6$ (*2′*); $\alpha_3 = \pi/3$ (*3′*); $\alpha_4 = \pi/2$(*4′*).

Fig. 5. Vertical pulse wave flux profiles of $\overline{u'w}$ (a) and $\overline{v'w}$ (b) at different values ofα angle for weak stratification: $\alpha_1 = 0$ (*1′*); $\alpha_2 = \pi/6$ (*2′*); $\alpha_3 = \pi/3$ (*3′*); $\alpha_4 = \pi/2$(*4′*).

Fig. 6. Vertical pulse wave flux profiles of $\overline{u'w}$ (a) and $\overline{v'w}$ (b) at different values ofα angle for very weak stratification: $\alpha_1 = 0$ (*1′*); $\alpha_2 = \pi/6$ (*2′*); $\alpha_3 = \pi/3$ (*3′*); $\alpha_4 = \pi/2$(*4′*).

Fig. 7. Dispersion curves of the first two modes of internal and subinertial waves at strong (a, b), weak (c) and very weak (d) stratification. The numbers of the subinertial wave modes are marked with a dash.

Fig. 8. Vertical wave flux profiles of momentum $\overline{u'w}$ atom internal (*1*) and subinertial waves (*2*) for strong (a), weak (b), and very weak (c) stratification;

the same fluxes only at the internal wave for three types of stratification (d).

Fig. 9. Vertical wave momentum flux profiles $\overline{v'w}$ at internal (*1*) and subinertial shafts (*2*) for strong (a), weak (b), and very weak (c) stratification; the same fluxes at the subinertial wave alone for the three types of stratification (d).

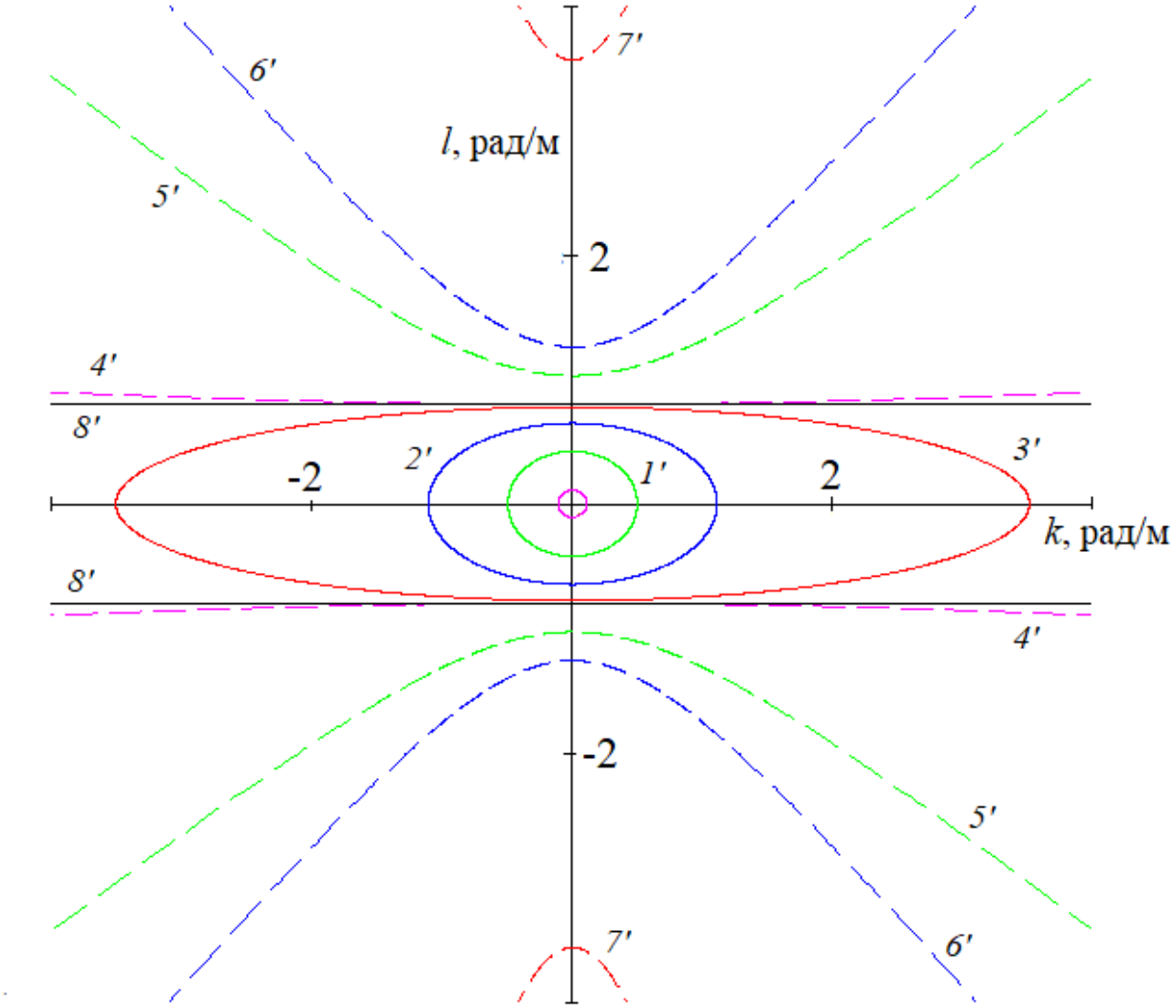

Fig. 1.

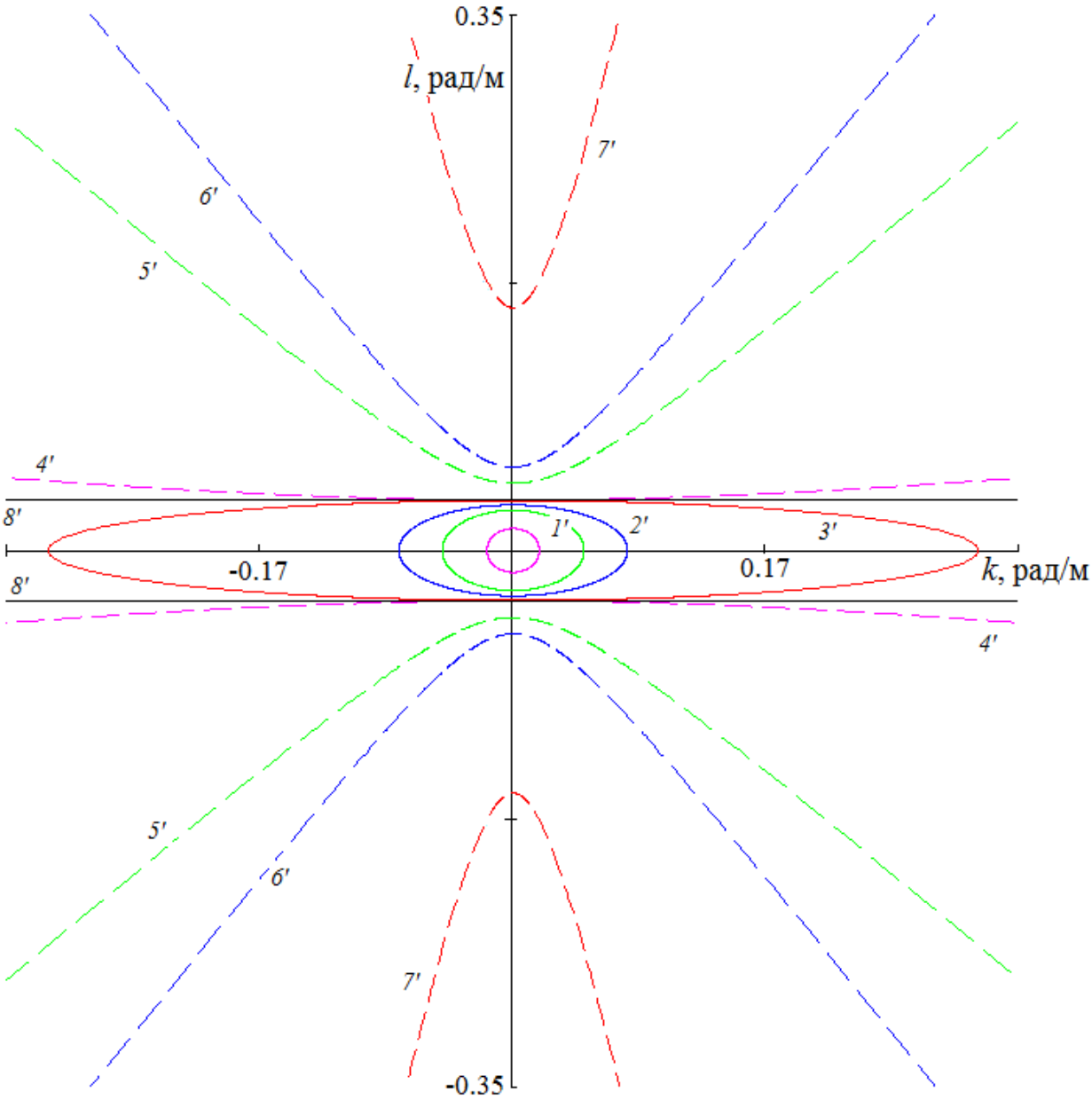

Fig. 2.

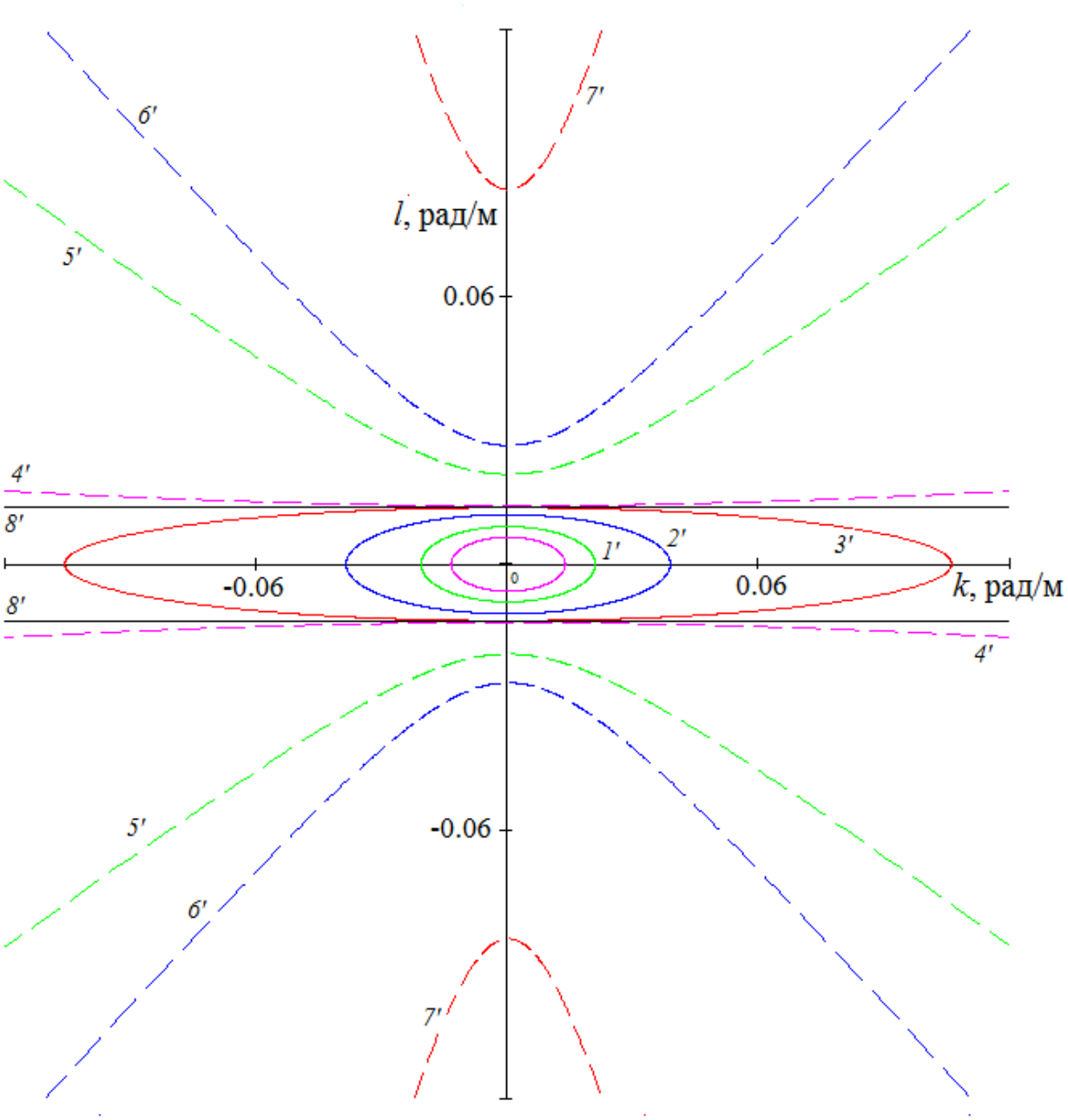

Fig. 3.

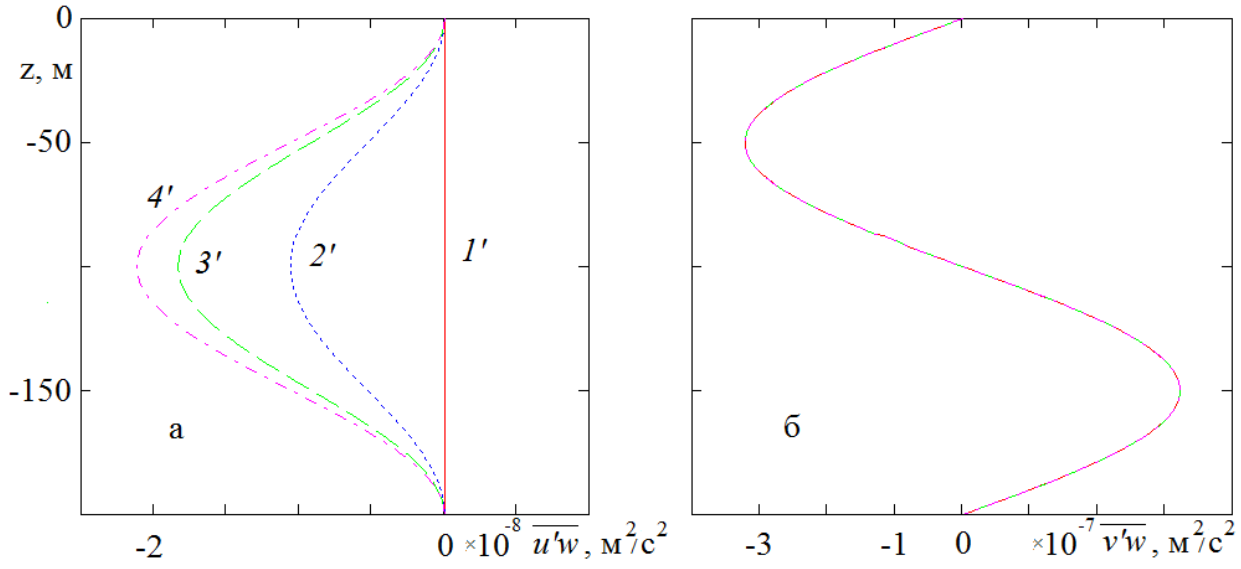
0
z, м
-50
-150
4′
3′
2′
1′
а
-2
0
×10-8 u′w, м2/с2
б
-3
-1
0
×10-7 v′w, м2/с2

Fig. 4.

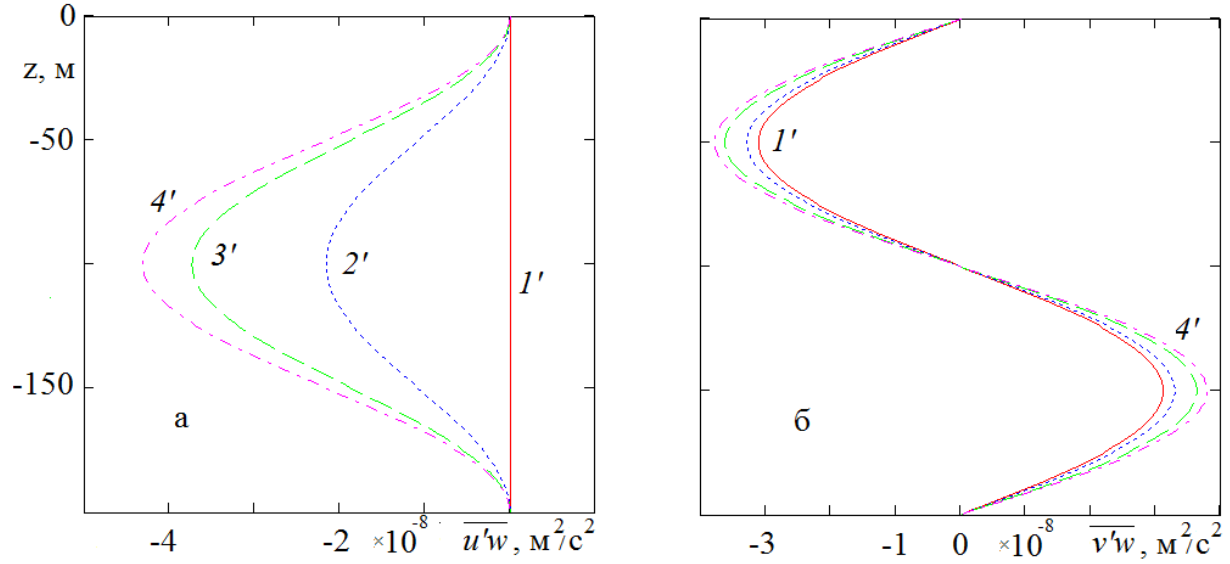
0
z, м
-50
-150
4′
3′
2′
1′
а
-4
-2
×10-8 u′w, м2/с2
1′
4′
б
-3
-1
0
×10-8 v′w, м2/с2

Fig. 5.

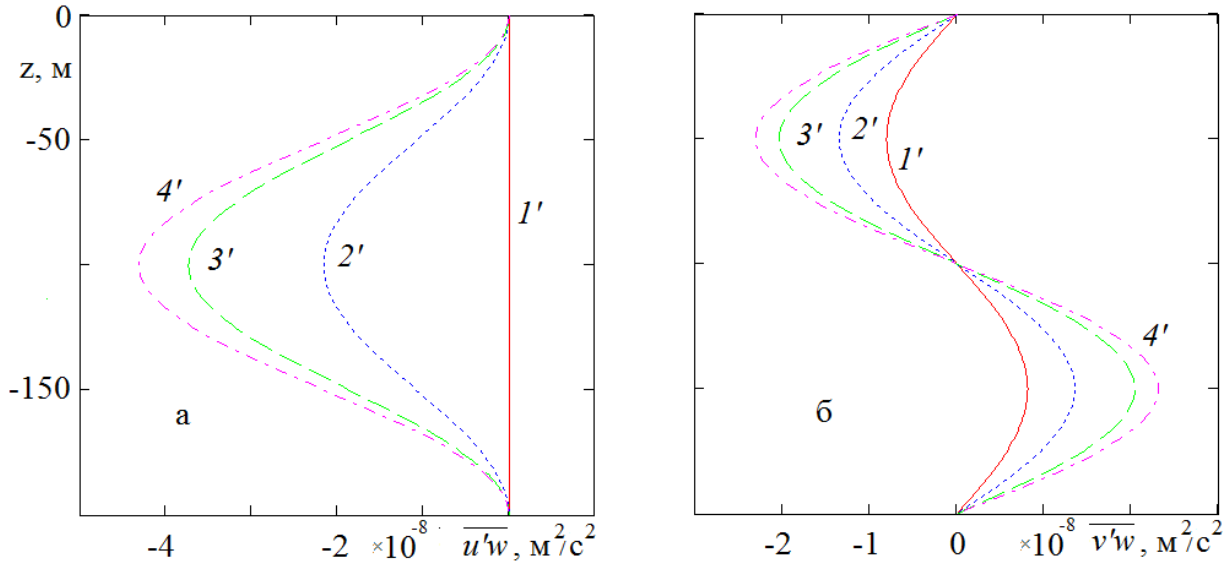
0
z, м
-50
-150
4′
3′
2′
1′
а
-4
-2
×10⁻⁸
u′w, м²/с²
3′
2′
1′
4′
б
-2
-1
0
×10⁻⁸
v′w, м²/с²

Fig. 6.

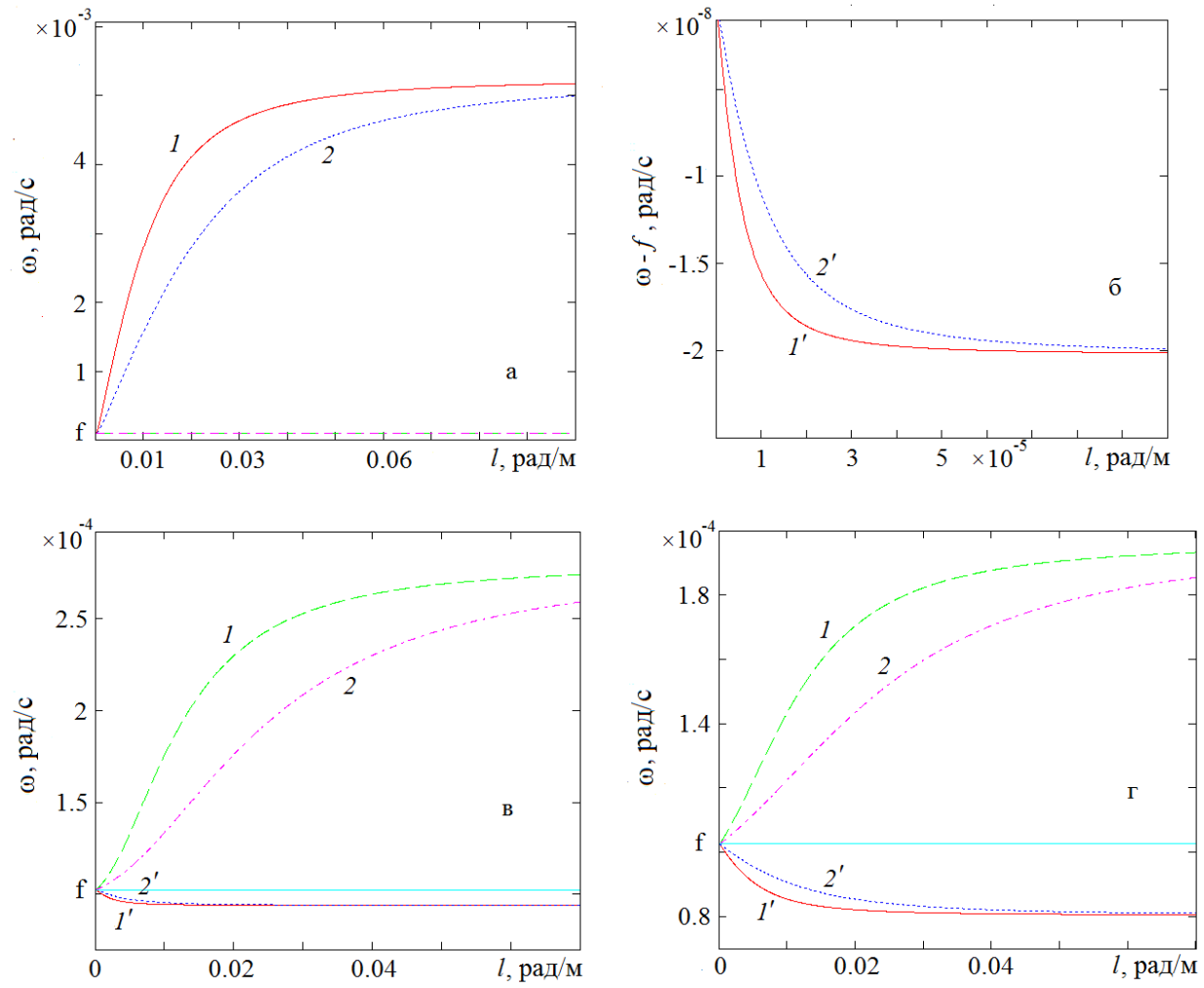
×10⁻³
ω, рад/с
4
2
1
f
1
2
а
0.01
0.03
0.06
l, рад/м
×10⁻⁸
ω - f, рад/с
-1
-1.5
-2
2′
1′
б
1
3
5
×10⁻⁵
l, рад/м
×10⁻⁴
ω, рад/с
2.5
2
1.5
f
1
2
2′
1′
в
0
0.02
0.04
l, рад/м
×10⁻⁴
ω, рад/с
1.8
1.4
f
0.8
1
2
2′
1′
г
0
0.02
0.04
l, рад/м

Fig. 7.

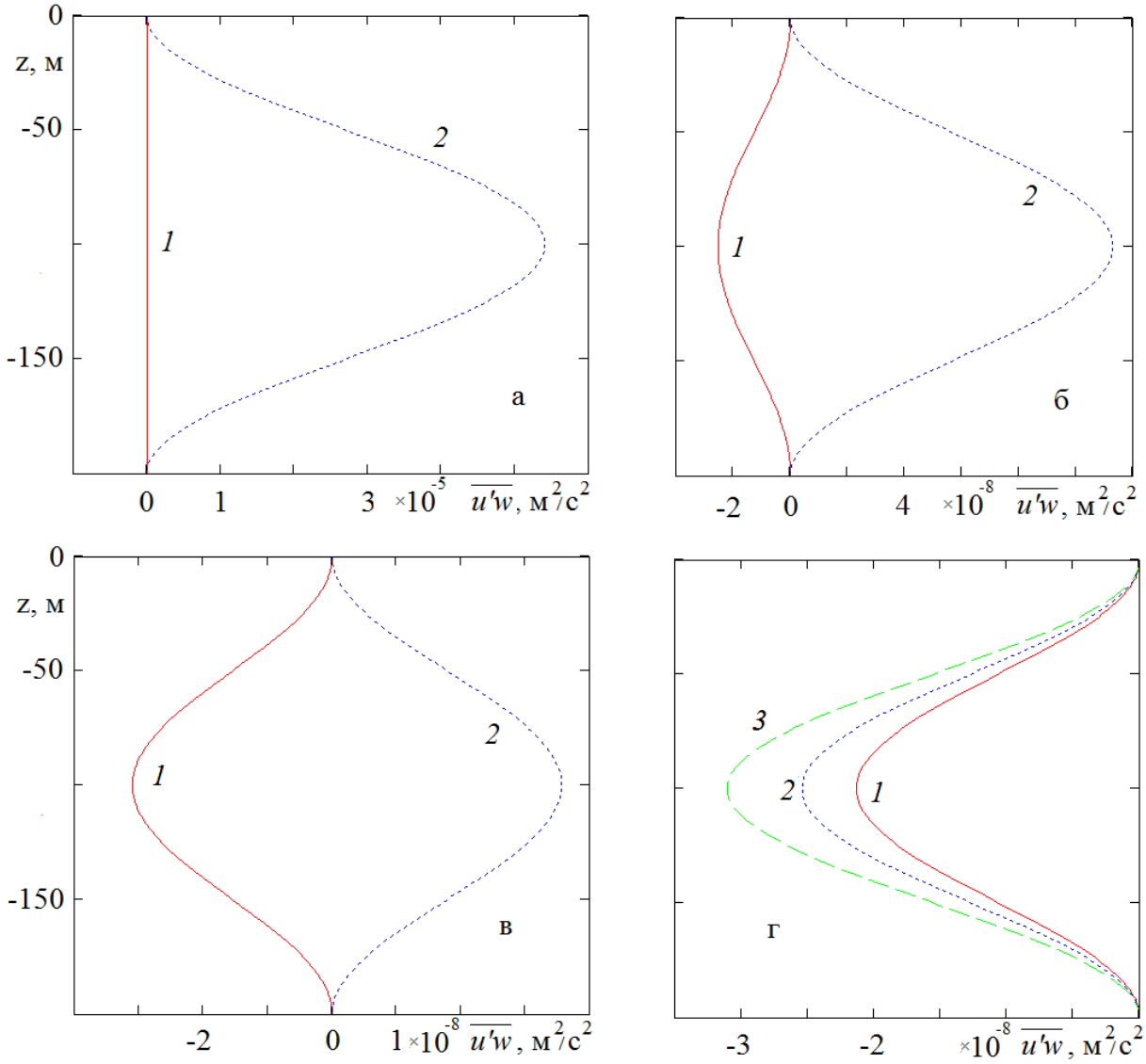

Fig. 8.

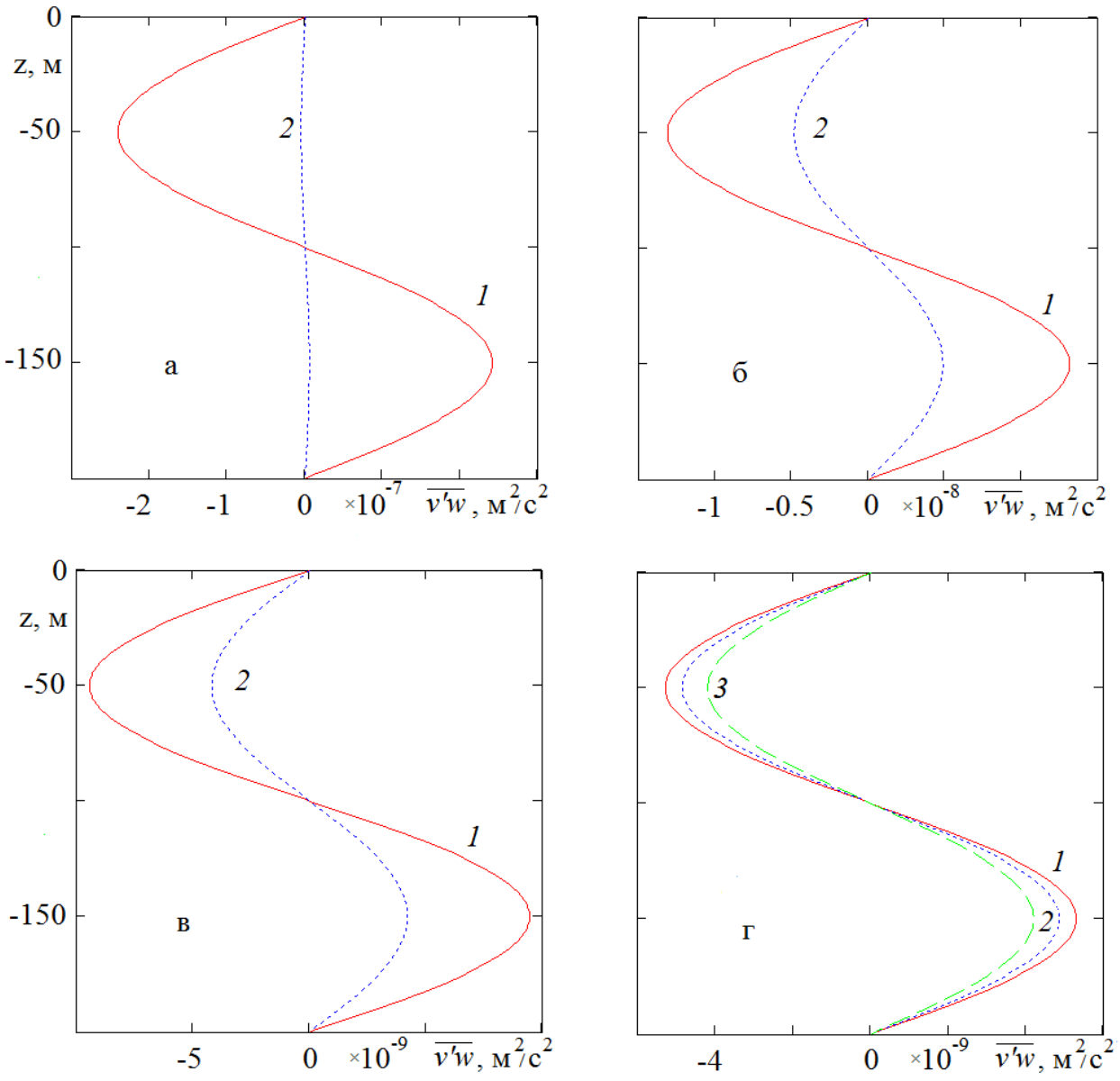

Fig. 9.